Voltage Mode Controller Design and Experimental Verification of a Three-Phase Capacitive-coupling Grid Connected Inverter in PV system

Chi-Wa Chao[1], Wai-Hei Choi[1], Chi-Seng Lam[2], Chi-Kong Wong[1], Ningyi Dai[1] and Man-Chung Wong[1,2]
1 - Department of Electrical and Computer Engineering, Faculty of Science and Technology, University of Macau, Macau, China
2 - State Key Laboratory of Analog and Mixed-Signal VLSI, University of Macau, Macau, China
E-mail: cslam@umac.mo / C.S.Lam@ieee.org

***Abstract*— In this paper, a voltage mode controller called Quasi proportional-resonant (Quasi-PR) controller has adopted in a three-phase capacitive-coupling grid-connected inverter (CGCI) PV system. Under CGCI structure, the function of the inverter is to compensate the reactive power as well as generate the active power to the grid with low operating dc-link voltage. The Quasi-PR controller could be effectively applied in a sinusoidal current tracking problem with low steady-state error and suppressing the system voltage disturbance at the fundamental frequency. Experimental results are given to verify the effectiveness of the suggested controller in CGCI.**

***Index Terms*— CGCI, Quasi-PR, Hysteresis, reactive power, pulse width modulation (PWM).**

I. Introduction

In traditional PV system, the inductive-coupling grid-connected inverter (IGCI) is generally applied to transfer to DC to AC active power to the grid. However, the operating voltage of the IGCI should be higher than the system voltage which means lower efficiency. Recently, the CGCI is proposed in PV system [1-2], which can compensate the reactive power as well as generate the active power to the grid with low operating dc-link voltage. Therefore, the functionality of the PV system can be enriched, it can be operated during daytime as well as night time.

Under the CGCI structure, most of the previous studies are focused on the parameter design or dc-link voltage control. For current tracking method, they usually apply the direct current tracking method, such as hysteresis pulse width modulation (PWM) due to its simplicity and fast response [3]. However, the drawback of the hysteresis PWM method is the variable switching frequency, thus an abundance of harmonic current with a wide range of switching frequency will inject to the grid to affect the system voltage. On the other hand, a bulky filter should be adopted in order to eliminate the induced harmonic current. Therefore, both the cost and physical size of the inverter will be increased.

Some of the researchers applied the indirect current tracking method in CGCI structure [1-2], [4], the voltage reference is calculated by a PI controller with current tracking error as input, then the switching signal can be achieved by the carrier based PWM method [5]. However, the PI controller is only effective when dealing with dc tracking problem, a large steady-state error will occur for sinusoidal reference tracking.

In this paper, the Quasi-PR controller is adopted in a three-phase CGCI PV system, the controller provides a resonant at the fundamental frequency, and thus the system voltage disturbance can be suppressed. Therefore, the Quasi-PR controller not only operates at a fixed switching frequency but also provide a better tracking performance than a traditional PI controller.

The operational principles of the CGCI in three-phase system will be given in Section II. Different type of voltage mode controller is introduced in Section III. Design of the Quasi-PR controller under CGCI is discussed in Section IV. Finally, experimental verification will be provided in Section V.

II. Operational Principles of CGCI in Three-Phase System

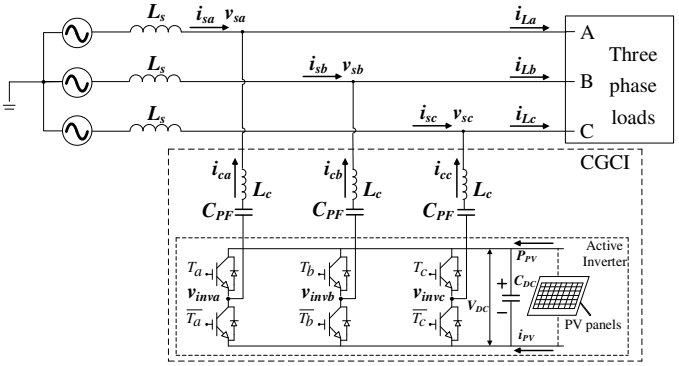

Fig. 1 Circuit configuration of CGCI.

The grid-connected inverter is to compensate the reactive power as well as generate the active power to the grid. Fig. 1

This work was supported in part by the Science and Technology Development Fund, Macao SAR (FDCT) (025/2017/A1, 109/2013/A3) and in part by the Research Committee of the University of Macau (MYRG2018-00039-FST, MYGR2017-00038-FST, MYRG2017-00090-AMSV).

shows the configuration of the CGCI, in which the inverter is connected to the grid through a coupling capacitor in series with an inductor. At fundamental frequency, the capacitor dominates the impedance which mainly compensates the inductive loading reactive power. The equivalent impedance is expressed as (1):

$$X_{LC} = -\frac{1}{2\pi f C_c} + 2\pi f L_c \tag{1}$$

In order to analyze the active power and reactive power provide by CGCI at the fundamental frequency, the injected active and reactive current to the grid is given by (2):

$$I_{cxf} = I_{cxfp} + j \cdot I_{cxfq} \tag{2}$$

where the subscript "*f*" denotes the fundamental frequency component; *x* represents *a,b,c* phase respectively, thus I_{cxfp} and I_{cxfq} are the fundamental injected active current and reactive current. Thus, the active and reactive power injected by CGCI in each phase is expressed as (3):

$$\begin{aligned} S_{cxf} &= V_{sxf} \cdot (I_{cxfp} - j \cdot I_{cxfq})^* \\ &= V_{sxf} \cdot \left(\frac{V_{invxf} - V_{sxf}}{jX_{LC}} \right)^* \\ &= V_{sxf} \cdot \left(\frac{V_{invxf} \sin\delta}{X_{LC}} + j\frac{V_{invxf} \cos\delta - V_{sxf}}{X_{LC}} \right) \\ &= \frac{V_{sxf} V_{invxf} \sin\delta}{X_{LC}} + j\left(\frac{V_{sxf} V_{invxf} \cos\delta - V_{sxf}^2}{X_{LC}} \right) \\ &= P_{cxf} + jQ_{cxf} \end{aligned} \tag{3}$$

where "*" denotes the conjugation, δ represent the angle between V_{invxf} and V_{sxf}. Based on (3), the relation of the inverter versus the grid voltage can be expressed as a ratio with regard to the active power and reactive power injection range is described as (4).

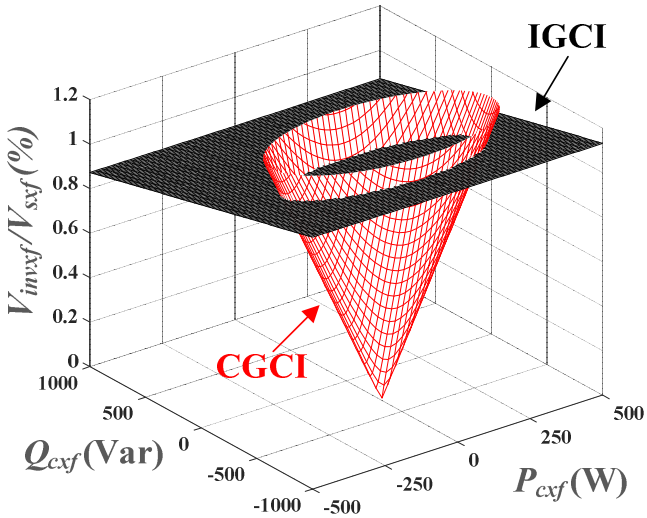

Fig. 2 The ratio of V_{invxf}/V_{sxf} in term of P_{cxf} and Q_{cxf} for IGCI and CGCI.

$$\frac{V_{invxf}}{V_{sxf}} = \sqrt{\left(\frac{P_{cxf}}{S_{base}}\right)^2 + \left(\frac{Q_{cxf}}{S_{base}} - 1\right)^2} \tag{4}$$

Where S_{base} is the base power of the CGCI and calculated as (5):

$$S_{base} = \frac{V_{sxf}^2}{X_{LC}} \tag{5}$$

According to (4), the normalized output voltage of CGCI with power flow variation is plotted with a three-dimension depiction in Fig. 2. Moreover, the power flow variation in IGCI is also plotted for comparison.

From Fig. 2, it can be observed that the CGCI attains lower inverter voltage (dc-link voltage) characteristic in some operating area compare to IGCI. The higher of the inverter voltage, the wider of the operating range of the CGCI. However, the operating range of the IGCI is wider than that in CGCI if the inverter higher than the grid voltage. Therefore, the CGCI structure is benefited when the required active and reactive power is within the mentioned operating area.

On the other hand, the CGCI can provide a fixed amount of reactive power when V_{invxf}/V_{sxf} is zero. Unlike the IGCI, the CGCI could provide the reactive power compensation during night time.

Since the inverter could provide reactive power and active power, a current reference is required to control the active inverter part. The instantaneous reactive and active theory can be applied (6)-(9) [6]:

$$\begin{bmatrix} v_\alpha \\ v_\beta \end{bmatrix} = \sqrt{\frac{2}{3}} \begin{bmatrix} 1 & -1/2 & -1/2 \\ 0 & \sqrt{3}/2 & -\sqrt{3}/2 \end{bmatrix} \begin{bmatrix} v_{sa} \\ v_{sb} \\ v_{sc} \end{bmatrix} \tag{6}$$

$$\begin{bmatrix} i_\alpha \\ i_\beta \end{bmatrix} = \sqrt{\frac{2}{3}} \begin{bmatrix} 1 & -1/2 & -1/2 \\ 0 & \sqrt{3}/2 & -\sqrt{3}/2 \end{bmatrix} \begin{bmatrix} i_{La} \\ i_{Lb} \\ i_{Lc} \end{bmatrix} \tag{7}$$

Clark transformation is applied in (6) and (7) to transform the voltage and current from *a-b-c* coordinates into *α-β* coordinates:

$$\begin{bmatrix} P_{\alpha\beta} \\ q_{\alpha\beta} \end{bmatrix} = \begin{bmatrix} v_\alpha & v_\beta \\ -v_\beta & v_\alpha \end{bmatrix} \begin{bmatrix} i_\alpha \\ i_\beta \end{bmatrix} = \begin{bmatrix} \bar{p} + \tilde{p} \\ \bar{q} + \tilde{q} \end{bmatrix} \tag{8}$$

where $\bar{p}$ and $\tilde{p}$ are the fundamental and ac components of the instantaneous active power of loading $P_{\alpha\beta}$. $\bar{q}$ and $\bar{q}$ are the fundamental and ac components of the instantaneous reactive power of loading $q_{\alpha\beta}$.

Since CGCI is capable to provide additional active power from the VSI, reference active power injection $V_{DC} \cdot i_{PV} = 3 \cdot P_{cxf}^*$ is inserted. Finally, the reference injected current is given by:

$$\begin{bmatrix} i_{ca}^{*} \\ i_{cb}^{*} \\ i_{cc}^{*} \end{bmatrix} = \sqrt{\frac{2}{3}} \frac{1}{v_{\alpha}^{2}+v_{\beta}^{2}} \begin{bmatrix} 1 & 0 \\ -1/2 & \sqrt{3}/2 \\ -1/2 & -\sqrt{3}/2 \end{bmatrix} \begin{bmatrix} v_{\alpha} & v_{\beta} \\ v_{\beta} & v_{\alpha} \end{bmatrix} \begin{bmatrix} \tilde{p}_{\alpha\beta}+3P_{cxf}^{*} \\ q_{\alpha\beta} \end{bmatrix} \quad (9)$$

In current tracking, the hysteresis PWM controller is normally applied to track the reference current. However, hysteresis PWM controller will introduce variable switching frequency, thus an abundance of harmonic current with a wide range of switching frequency will inject to the grid to affect the system voltage. On the other hand, a bulky filter should be adopted in order to eliminate the induced harmonic current. Therefore, both the cost and physical size of the inverter will be increased.

Therefore, a voltage mode controller with a fixed switching frequency is suggested and discussed in the next section.

III. VOLTAGE MODE CONTROLLER FOR CGCI

The control block diagram of the overall system in s-domain is shown in Fig. 3. And the overall closed-loop transfer function is written as (10).

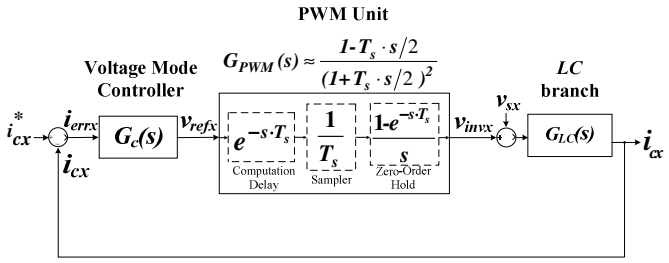

Fig. 3 Overall control block diagram of CGCI

$$i_{cx}(s) = \frac{G_C(s)G_{PWM}(s)G_{LC}(s)}{G_C(s)G_{PWM}(s)G_{LC}(s)+1} i_{cx}^{*}(s) - \frac{G_{LC}(s)}{G_C(s)G_{PWM}(s)G_{LC}(s)+1} v_{sx}(s) \quad (10)$$

Where G_C, G_{PWM} and G_{LC} represent the transfer function of the voltage model controller, PWM controller and the LC impedance respectively.

For the voltage mode controller, the different type of control methods can be applied, such as PI, PR, and Quasi-PR controller.

a. Proportional Integral (PI)

PI control is one of a widely used voltage mode feedback control in industrial application and its s-domain expression is shown in (11). k_p represents the proportional gain and k_i represents integral gain. Although PI controller offers theoretical large amplification to the reference signal in signal tracking, it is not capable to track sinusoidal reference signals and low capability in disturbance rejection.

$$G_{PI}(s) = k_p + \frac{k_i}{s} \quad (11)$$

Since the integral term is slow reacting to the signal, it cannot eliminate steady-state errors in sinusoidal signal tracking and slow response to the transient signal variation. In addition, if the amplification of PI control is too large, it also increases the sensitivity of the system and the system will be easily become unstable.

b. Proportional Resonant (PR)

Proportional-resonant (PR) controller theoretical has almost the same steady-state error situation and transient performance as PI control. It provides infinite gain at the resonant frequency and results in perfect signals tracking at this resonant frequency. Its s-domain expression is shown in (12).

$$G_{PR} = k_p + \frac{k_r s}{s^2+\omega_0^2} \quad (12)$$

Where the k_r is resonant gain and ω_0 is resonant angular frequency. However, the infinite amplification is difficult to realize either for the digital signal processor. Furthermore, PR control cannot present large amplification when the system operating frequency varies from the resonant frequency.

c. Quasi-Proportional Resonant (Quasi-PR)

A quasi-PR controller not only ensures the stability problem regarding the PR controller infinite gain but also allow slight frequency variation. Its s-domain expression is given in (13).

$$G_{Quasi\text{-}PR} = k_p + \frac{k_r s}{s^2+2\omega_c s+\omega_0^2} \quad (13)$$

The additional term of is resonant angular frequency. Quasi-PR can introduce a high gain that can eliminate steady-state errors around the resonant frequency, which is possible to implement through the digital signal processor (DSP). In addition, the characteristics of Quasi-PR can highly mitigate the frequency disturbance of the grid. Therefore, Quasi-PR is best candidate among the mentioned controller.

IV. QUASI-PR CONTROLLER

The adopted Quasi-PR controller can optimize the dynamic reference tracking and anti-interference capabilities of HGCI. There are three parameters (k_p, k_r and ω_c) required to be designed for the controller. The design criteria can be summarized the followings:

- An appropriate ω_c can provide enough preventing frequency variation capability around the resonant frequency;
- k_r should be designed to obtain a high enough gain at the resonant frequency to eliminate current tracking error;
- k_p should be designed to optimize the stability and anti-interference of the system.

After the parameter of the Quasi-PR controller was determined, the blot-plot analysis is carried out in both PI and Quasi-PR controller. The signal amplification at the fundamental frequency and anti-disturbance capabilities with PI and Quasi-PR controllers are also put in comparison. The bold-plot diagram of $G_i(s) = G_c(s)G_{PWM}(s)G_{LC}(s)$ is shown in Fig. 4, the Quasi-PR controller can provide a significant high amplification at the fundamental frequency rather than PI controller just provide a smooth and low signal amplification. On the other hand, the bode-plot diagram of $G_j(s) = \frac{G_{LC}(s)}{G_c(s)G_{PWM}(s)G_{LC}(s)+1}$ with PI and Quasi-PR controllers is shown in Fig. 5, there is a significant resonant frequency at the fundamental frequency, which means the controller can significantly suppress the disturbance of the grid voltage $v_{sx}(s)$.

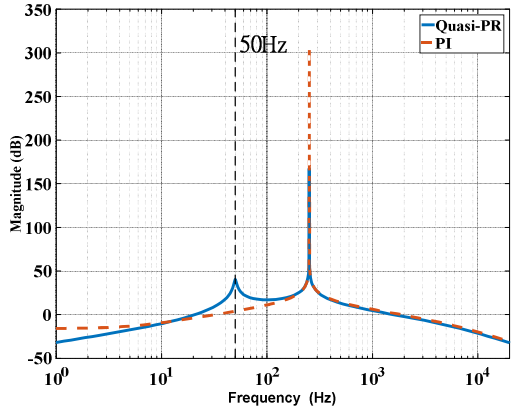

Fig. 4 Bode-plot diagram of $G_i(s)$ with PI and Quasi-PR controllers.

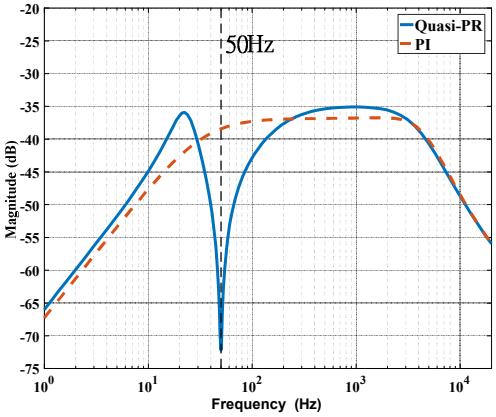

Fig. 5 Bode-plot diagram of $G_j(s)$ with PI and Quasi-PR controllers.

V. Hardware Verification

To verify the effectiveness of Quasi-PR controller in three-phase CGCI system, experimental results are given in this section. Table I lists the parameters of the CGCI and the load, the CGCI is supported by a DC power source to emulate PV system. The inverter is being operated to compensate the load reactive power at round 1.0 kvar, at a meanwhile to support a portion of active power 200W to the load, thus release the transmission loss from the grid to the load.

TABLE I. Hardware System Parameter

Item	Value
Grid voltage V_s	110~115 Vrms, 50 Hz
Filter inductor L	5 mH
Coupling capacitor C	80uF
DC-link voltage	50 V
Active power transfer	200 W
Linear load	16.3 Ω, 40.0 mH

Fig. 6 shows the three-phase grid voltage and source current waveform before and after compensation by the CGCI: (a) loading; (b) CGCI with hysteresis PWM method; (c) CGCI with PI controller; (d) CGCI with Quasi-PR controller. From Fig 6 (b), a high ripple current occurs in the source current even after the grid voltage which is induced by the hysteresis PWM by the CGCI. From Fig. 6 (c), the CGCI current tracking performance under PI controller is unacceptable, large current distortion is introduced and becomes unstable. In Fig. 6 (d), under Quasi-PR control method, both active and reactive power can track with its reference accordingly. Table II summarized the steady-state performance among the three control methods, which is focused on the three aspects source current THD (THD_{is}), active power tracking error (P_{error}) and reactive power tracking error (Q_{error}). From Table II, it can be observed that the Quasi-PR controller is the most suitable one for the CGCI system.

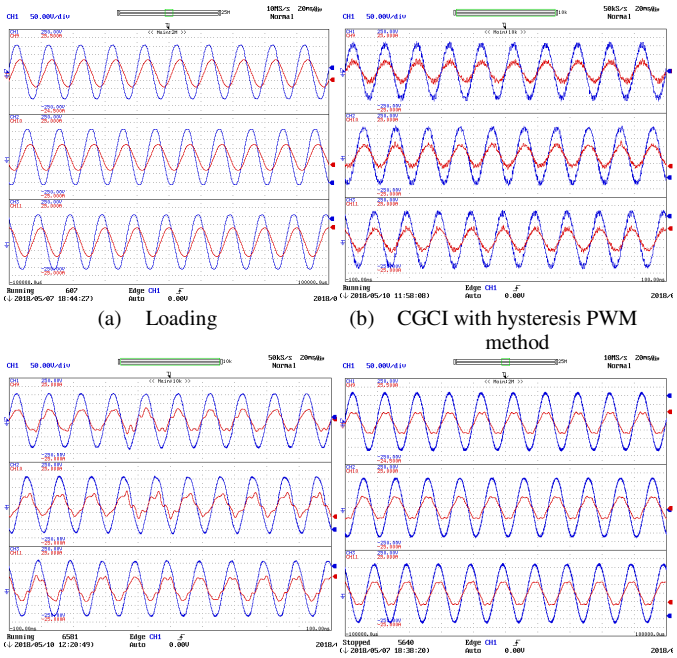

(a) Loading (b) CGCI with hysteresis PWM method

(c) CGCI with PI controller (d) CGCI with Quasi-PR controller

Fig. 6 voltage and current waveform for CGCI under different controllers.

TABLE II Steady-State Performance Using Hysteresis, PI and PR Controller

Controller	*THD_is (%)*	*P_ref (W)*	*P_inj (W)*	*Q_load (var)*	*Q_inj (var)*	*P_error (%)*	*Q_error (%)*
Hysteresis	18.1	200	70	1080	970	65.0	10.2
PI	22.5	200	150	1080	1050	25.0	2.8
Qusai PR	9.7	200	170	1080	980	15.0	9.3

VI. CONCLUSION

In this paper, Quasi-PR voltage mode controller is verified and implemented in a three-phase CGCI PV system. According to the theoretical studies and experimental verification, the adopted Quasi-PR controller shows the best performance among the mentioned controllers, the Quasi-PR controller could be effectively applied in a sinusoidal current tracking problem with low steady-state error and suppressing the system voltage disturbance at the fundamental frequency.

V. REFERENCES

[1] T. Ye, N. Dai, C. S. Lam, M. C. Wong and J. M. Guerrero, "Analysis, design, and implementation of a quasi-proportional-resonant controller for a multifunctional capacitive-coupling grid-connected inverter," *IEEE Trans. Industrial Application*, vol. 52, no. 5, pp. 4269-4280, Oct. 2016.

[2] N. Y. Dai, W. C. Zhang, M. C. Wong, J. M. Guerrero and C. S. Lam, "Analysis, control and experimental verification of a single-phase capacitive-coupling grid-connected inverter," *IET Power Electron.*, vol. 8, no. 5, pp. 770-782, 5 2015.

[3] S.H. Li, C.M. Liaw, "On the DSP-based switch-mode rectifier with robust varying-band hysteresis PWM scheme", *IEEE Trans. on Power Electronics*, vol. 19, no. 6, pp. 1417-1425, Nov. 2004.

[4] L. Wang, C. S. Lam and M. C. Wong, "A Hybrid STATCOM with wide compensation range and low dc-link voltage", *IEEE Trans. on Industrial Electronics*, vol. 63, no. 6, pp. 3333 – 3343, Jun. 2016.

[6] H. Akagi, Y. Kanazawa, and A. Nabae, "Generalized theory of the instantaneous reactive power in three-phase currents," *Internation Power Electronics Conference*, 1983, pp. 1375-1386.